Sensory tuning does not match behavioral relevance of communication signals in free-living weakly electric fish

Jörg Henninger[1], Rüdiger Krahe[2,3], Frank Kirschbaum[2], Jan Grewe[1], Jan Benda[1†]

[1] Institut für Neurobiologie, Eberhard Karls Universität, Auf der Morgenstelle 28E, 72076 Tübingen, Germany

[2] Lebenswissenschaftliche Fakultät, Humboldt-Universität zu Berlin, Philippstr. 13, 10115 Berlin, Germany

[3] McGill University, Department of Biology, 1205 Ave. Docteur Penfield, Montreal, Quebec H3A 1B1, Canada

[†] corresponding author: jan.benda@uni-tuebingen.de

Abstract

Sensory systems evolve in the ecological niches each species is occupying. Accordingly, the tuning of sensory neurons is expected to match the statistics of natural stimuli. For an unbiased quantification of sensory scenes we tracked natural communication behavior of the weakly electric fish *Apteronotus rostratus* in their Neotropical rainforest habitat with high spatio-temporal resolution over several days. In the context of courtship and aggression we observed large quantities of electrocommunication signals. Echo responses and acknowledgment signals clearly demonstrated the behavioral relevance of these signals. Despite their relevance these signals are non-optimally represented in the sensory periphery. Frequencies of courtship signals are far outside of the neurons' best tuning range and signals occurring in assessment and attack behaviors drive sensory neurons just above threshold. Our results emphasize the importance of quantifying sensory scenes derived from freely behaving animals in their natural habitats for understanding the evolution and function of neural systems.

Introduction

Sensory systems evolve in the context of species-specific natural sensory scenes (Lewicki et al., 2014). Consequently, naturalistic stimuli have been crucial for advances in understanding the design and function of neural circuits in sensory systems, in particular the visual (Laughlin, 1981; Olshausen and Field, 1996; Betsch et al., 2004; Gollisch and Meister, 2010) and the auditory system (Theunissen et al., 2000; Smith and Lewicki, 2006; Clemens and Ronacher, 2013). Communication signals are natural stimuli that are, by definition, behaviorally relevant (Wilson, 1975). Not surprisingly, acoustic communication signals, for example, have been reported to evoke responses in peripheral auditory neurons that are highly informative about these stimuli (Rieke et al., 1995; Machens et al., 2005). However, other stimulus ensembles that do not optimally drive sensory neurons may also be behaviorally relevant and equally important for understanding the functioning of neural systems. Unfortunately, they are often neglected from an electrophysiological point of view, because they do not evoke obvious neural responses (Olshausen and Field, 2005).

To avoid this bias, we first describe behaviorally relevant sensory scenes in an animal's natural habitat and then compare the estimated resulting stimulus properties with known tuning characteristics of the respective sensory system. Tracking freely behaving and unrestrained animals in natural environments is notoriously challenging (Rodriguez-Munoz et al., 2010). We took advantage of the continuously generated electric organ discharge (EOD; Fig. 1 A) of gymnotiform weakly electric fish (Heiligenberg, 1991), to track their movements and electrocommunication signals without the need of tagging individual fish.

The quasi-sinusoidal EOD together with an array of electroreceptors distributed over the fish's skin (Carr et al., 1982) forms an active electrosensory system used for prey capture (Nelson and MacIver, 1999), navigation (Fotowat et al., 2013), and communication (Smith, 2013). Both, the EOD alone and its modulations, function as communication signals that convey information about species, sex, status and intent of individuals (Hagedorn and Heiligenberg, 1985; Stamper et al., 2010; Fugère et al., 2011). In *Apteronotus* several types of brief EOD frequency excursions called "chirps"(Fig. 1 B) have been studied extensively in the laboratory (Engler and Zupanc, 2001; Zakon et al., 2002) and have been associated with courtship (Hagedorn and Heiligenberg, 1985) and aggression (Hupé and Lewis, 2008). P-unit tuberous electroreceptors encode amplitude modulations of the EOD arising in communication contexts (Bastian, 1981a). Their frequency tuning is crucial for the encoding of chirps (Benda et al., 2005; Walz et al., 2014).

We describe, for the first time, electrocommunication behavior of weakly-electric fish recorded in their natural neotropical habitat with high temporal and spatial resolution. We found extensive chirping interactions on

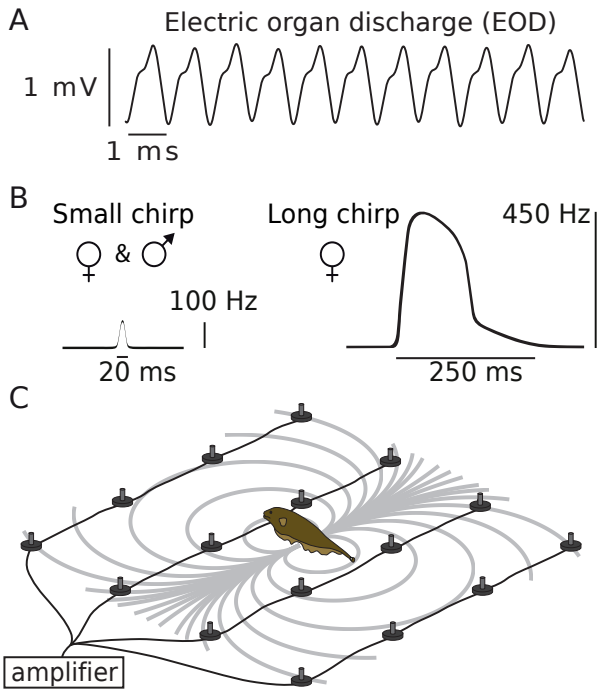

Figure 1: Monitoring electrocommunication behavior in the natural habitat. A) EOD waveform of *A. rostratus*. B) Transient increases of EOD frequency, called small and long chirps, function as communication signals. C) The EOD generates a dipolar electric field (gray isopotential lines) that we recorded with an electrode array, allowing to monitor fish interactions with high temporal and spatial acuity.

timescales ranging from tens of milliseconds to minutes in the context of courtship. In a complementary breeding experiment we confirmed the synchronizing role of chirping in spawning. Surprisingly, we found a strong mismatch between properties of courtship signals extracted from our outdoor recordings and the frequency tuning of the respective P-type electroreceptor afferents recorded in electrophysiological experiments. Our data demonstrate that receptor neurons do not have to be optimally tuned to relevant stimuli and that sensory systems are very well able to process non-optimal but relevant stimuli.

Results

We recorded the EODs of weakly electric fish in a stream in the Panamanian rainforest by means of a submerged electrode array at the onset of their reproductive season in May, 2012 (Fig. 1 C, Fig. S 1, movie S 4). Individual gymnotiform knifefish, *Apteronotus rostratus*, were identified and their movements tracked continuously based on the species- and individual-specific frequency of their EOD (EODf=600 to 1200 Hz). In these recordings we detected several types of "chirps" emitted during courtship and aggression (Fig. 1 B). This approach allowed us

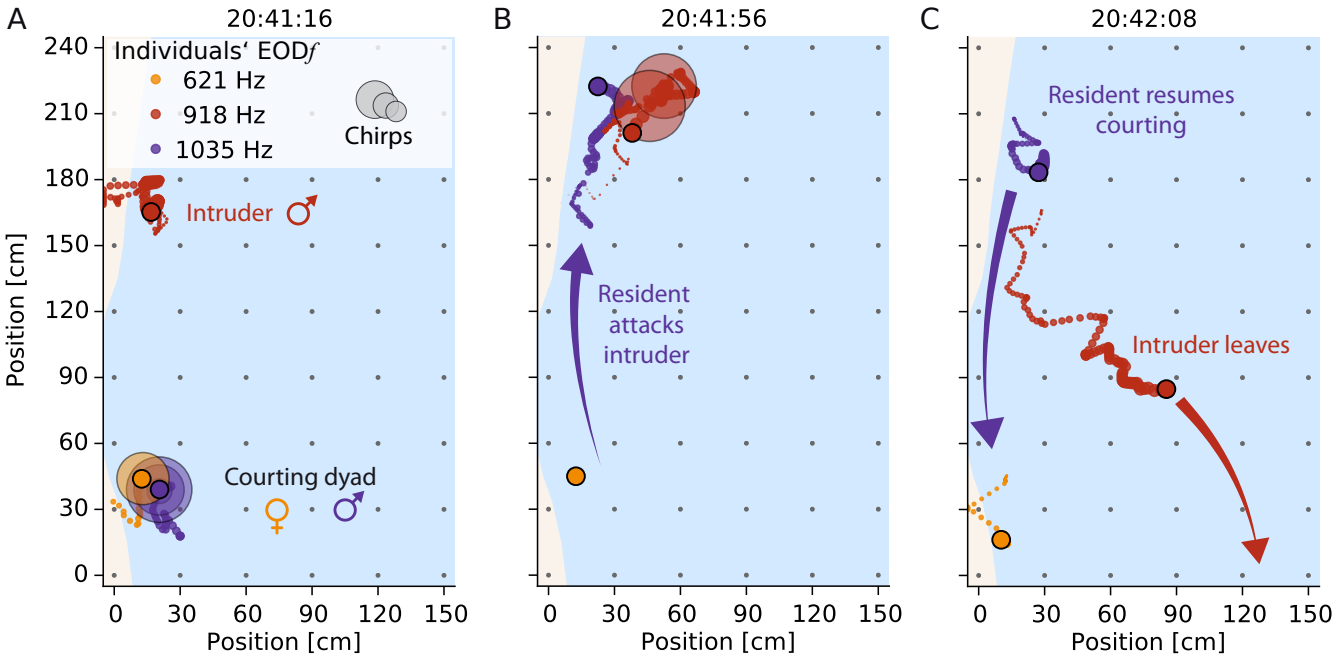

Figure 2: Snapshots of reconstructed fish interactions. See movie S 5 for an animation. The current fish position is marked by filled circles. Trailing dots indicate the positions over the preceding 5 s. Colors label individual fish throughout the manuscript. Large transparent circles denote occurrence of chirps. Gray dots indicate electrode positions, and light blue illustrates the water surface. The direction of water flow is from top to bottom. A) Courting female (orange) and male (purple) are engaged in intense chirping activity. An intruder male (red) lingers at a distance of about one meter. B) The courting male attacks (purple arrow) the intruder who emits a series of chirps and, C) leaves the recording area (red arrow), while the resident male resumes courting (red arrow).

to reconstruct social interactions in detail (Fig. 2, movies S 5 and S 6) and evaluate the associated sensory scenes experienced by these fish in their natural habitat.

Electrocommunication in the wild We focused on two relevant communication situations, i.e., courtship and aggressive dyadic interactions. In total, we detected 54 episodes of short-distance interactions that we interpreted as courtship (see below) between low-frequency females (EODf $<$ 750 Hz, n=2) and high-frequency males (EODf $>$ 750 Hz, $n = 6$), occurring in 2 out of 5 nights. Courting was characterized by extensive production of chirps (Fig. 2 A) by both males and females — with up to 8 400 chirps per individual per night. Most chirps were so-called "small chirps", characterized by short duration ($<$ 20 ms) EODf excursions of less than 150 Hz and minimal reduction in EOD amplitude (Engler and Zupanc, 2001) (Fig. 1 B and Fig. 3). Only females emitted an additional type of chirp in courtship episodes, the "long chirp" (Fig. 1 B and Fig. 3), with a duration of 162 ± 39 ms ($n = 54$), a

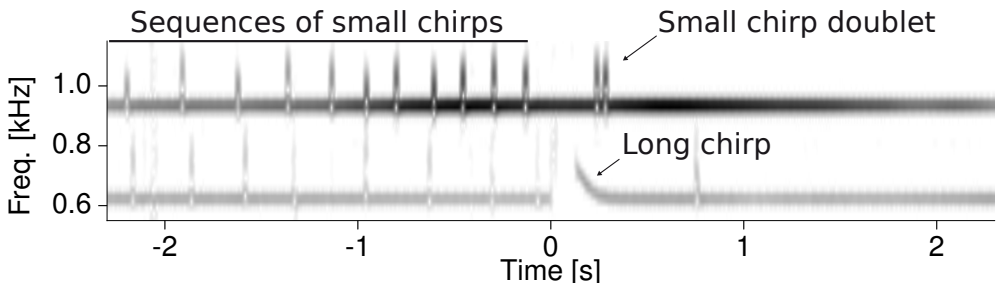

Figure 3: Spectrogram of stereotyped courtship chirping. The spectrogram (audio S 3) shows EODfs of a female (620 Hz, same as in Fig. 2) and a male (930 Hz) and their stereotyped chirping pattern during courtship: the two fish concurrently produce series of small chirps before the female generates a long chirp and the male responds with a chirp-doublet.

large EODf excursion of about 400 Hz, and a strong decrease in EOD amplitude. Per night and female we observed 9 and 45 long chirps, respectively, generated every 3 to 9 minutes (1st and 3rd quartile), between 7 pm and 1 am (Fig. 4 A). Occasionally, courtship was interrupted by intruding males, leading to aggressive interactions between resident and intruder males (see below).

Courtship chirping Roaming males approached and extensively courted females by emitting large numbers of small chirps. Courtship communication was highly structured, with female long chirps playing a central role. Long chirps were preceded by persistent emission of small chirps by the male with rates of up to 3 Hz (Figs. 5 A, C). Immediately before the long chirp, the female small-chirp rate tripled from below 1 Hz to about 3 Hz within a few seconds. The male chirp rate followed this increase until the concurrent high-frequency chirping of both fish ceased after the female long chirp. These chirp episodes were characterized by close proximity of the two fish ($<$ 30 cm, Figs. 5 B, D). Long chirps were consistently acknowledged by males with a doublet of small chirps emitted 229 ± 31 ms after long chirp onset (Fig. 3). The two chirps of the doublet were separated by only 46 ± 6 ms, more than seven-fold shorter than the most prevalent chirp intervals (Fig. S 2). The concurrent increase in chirp rate and its termination by the female long chirp and male doublet stood out as a highly stereotyped communication motif that clearly indicates fast interactive communication (Fig. 3, audio S 3).

Males echo female chirps On a sub-second timescale, male chirping was modulated by the timing of female chirps (Figs. 6 A, C). Following a female small chirp, male chirp probability first decreased to a minimum at about 75 ms (significant in 4 out of 5 pairs of fish) and subsequently increased to a peak at about 165 ms (significant in 4 out of 5 pairs of fish). In contrast to males, females did not show any echo response (Figs. 6 B, D) — they timed their chirps independently of the males' chirps.

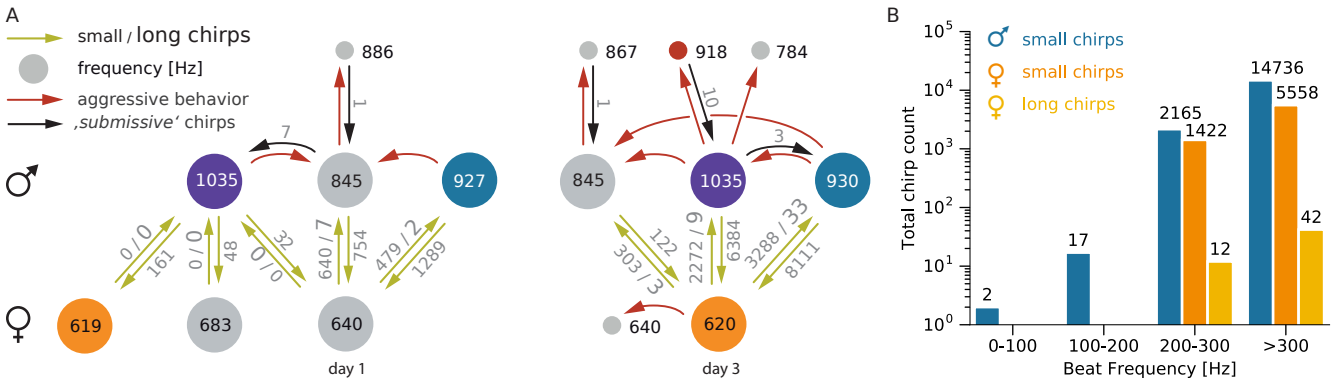

Figure 4: Social interactions and chirping. A) Ethogram of interacting *A. rostratus* individuals (colored circles) displaying their social relationships based on data from 2012-05-10 (night 1) and 2012-05-12 (night 3). The numbers within circles indicate the EOD*f*s of each fish in Hertz. Fish with similar EOD*f*s on day 1 and day 3 may have been the same individuals. Green arrows and associated numbers indicate the numbers of small chirps and long chirps emitted in close proximity (< 50 cm). Red arrows indicate aggressive behaviors, and black arrows the number of small chirps emitted during aggressive interactions. B) Histogram of chirp counts as a function of beat frequency (bin-width: 100 Hz). Note logarithmic scale used for chirp counts.

Competition between males A second common type of electro-communication interaction observed in our field data was aggressive encounters between males competing for access to reproductively active females. These aggressive interactions were triggered by intruding males that disrupted courtship of a resident, courting dyad. Resident males detected and often attacked intruders over distances of up to 177 cm, showing a clear onset of directed movement toward the intruder (Fig. 2 C, movie S 5). In 5 out of 12 such situations a few small chirps indistinguishable from those produced during courtship were emitted exclusively by the retreating fish (Fig. 4 A). We observed a single rise, a slow increase in EOD*f* (Zakon et al., 2002), emitted by a retreating intruder fish.

Synchronization of spawning We investigated the role of the female long chirp in a breeding experiment in the laboratory (Kirschbaum and Schugardt, 2002) by continuously recording and videotaping a group of 3 males and 3 females of the closely related species *A. leptorhynchus* (de Santana and Vari, 2013) over more than 5 months. Scanning more than 1.3 million emitted chirps, we found 76 female long chirps embedded in communication episodes closely similar to those observed in *A. rostratus* in the wild (compare Fig. 7 B with Fig. 3). Eggs were only found after nights with long chirps (six nights). The number of eggs found corresponded roughly to the number of observed long chirps, supporting previous anecdotal findings that *Apteronotus* females spawn single eggs during courtship episodes (Hagedorn and Heiligenberg, 1985). The associated video sequences triggered on female long chirps show that before spawning females swim on their side close to the substrate, e.g., a rock or a filter, while

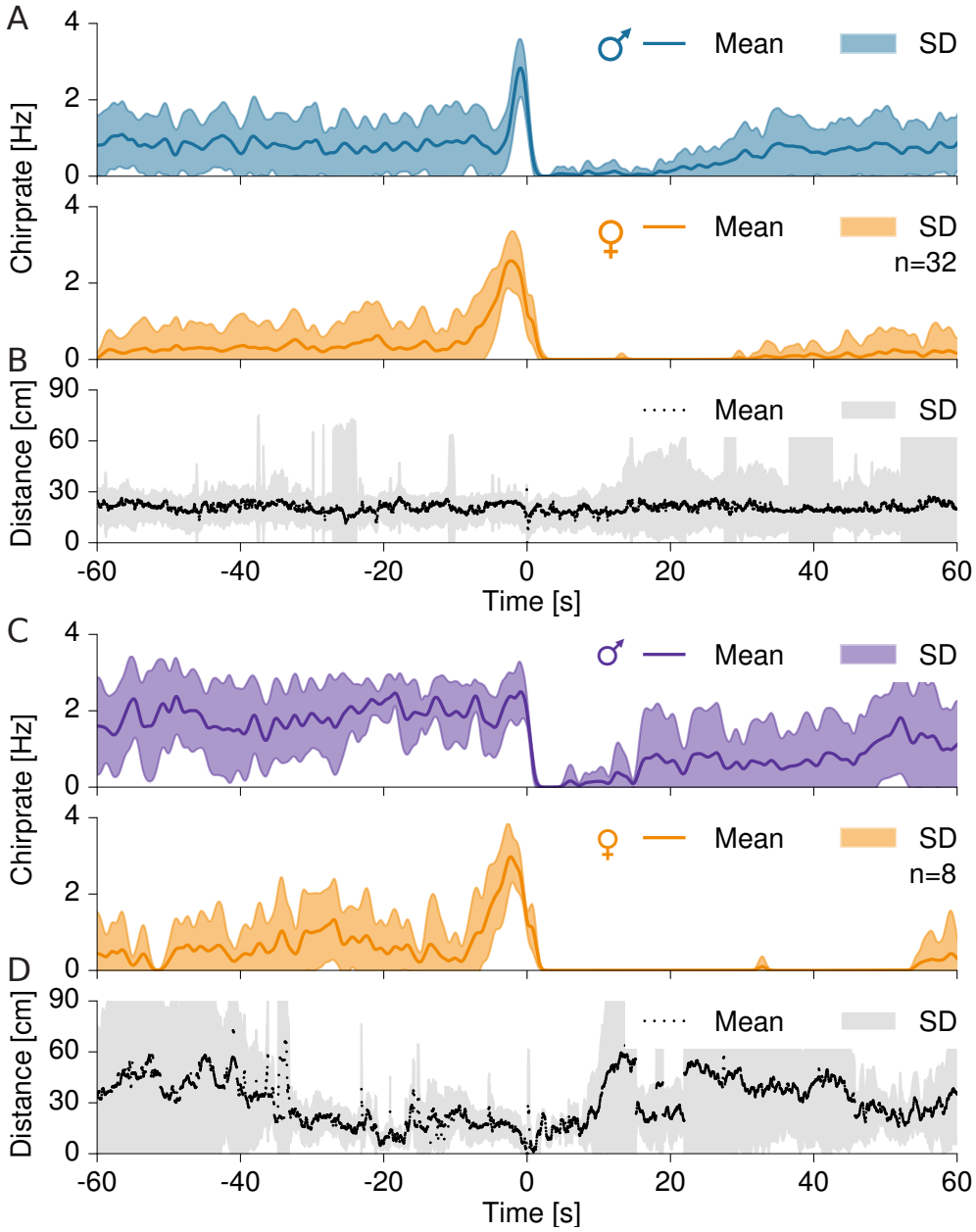

Figure 5: Temporal structure of courtship chirping of two example pairs. A) Average rate of small chirps of a male (top, EODf = 930 Hz) courting a female (bottom, EODf = 620 Hz, same pair as in Fig. 3, beat frequency is 310 Hz). B) Corresponding distance between the courting male and female. C, D) Same as in A and B for the pair shown in Fig. 2 (same female, male EODf = 1035 Hz, beat frequency 415 Hz). Time zero marks the female long chirp. Bands mark SD.

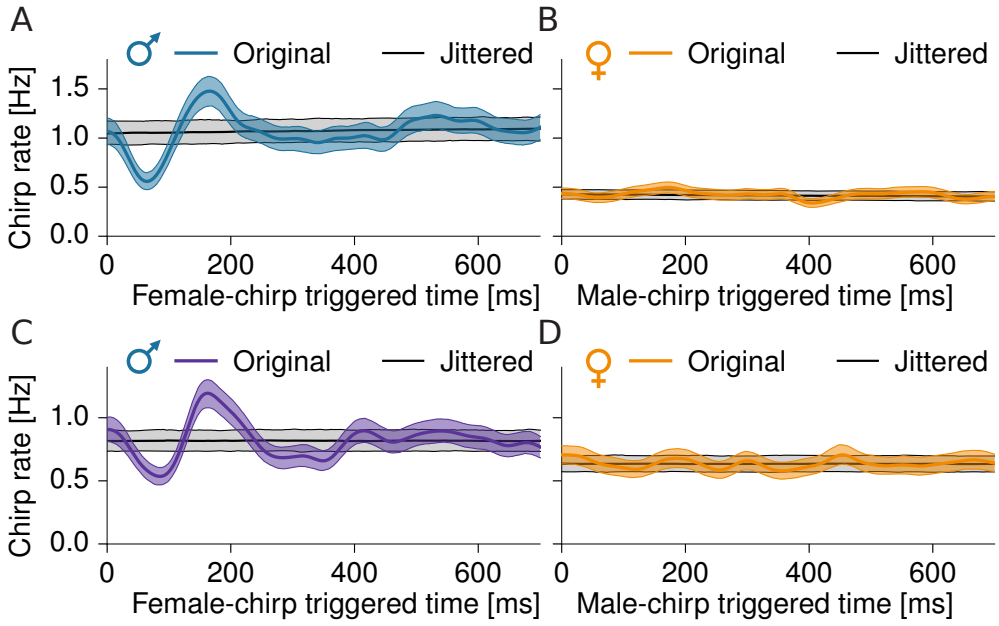

Figure 6: Fine structure of courtship chirping. Shown are cross-correlograms of chirp times, i.e. chirp rate of one fish relative to each chirp of the other fish (median with 95 % confidence interval in color), of the same courting pairs of fish as in Fig. 5. Corresponding chirp rates and confidence intervals from randomly jittered, independent chirp times are shown in gray. A, C) Male chirping is first significantly inhibited immediately after a female chirp (A: at 64 ms, Cohen's $d = 9.3$, C: at 85 ms, Cohen's $d = 7.1$) and then transiently increased (A: at 166 ms, $d = 5.9$, C: at 162 ms, $d = 7.5$). B, D) Female chirps are timed independently of male chirps (B: maximum $d = 2.8$, D: maximum $d = 1.9$).

the male hovers in the vicinity of the female and emits chirps continuously (movie S 7). In the last seconds before spawning, the female starts to emit a series of chirps, whereupon the male approaches the female. A fraction of a second before the female emits its long chirp, the male pushes the female and retreats almost immediately afterwards (Fig. 7). It seems highly likely that this short episode depicts the synchronized release of egg and sperm.

Mismatch between sensory tuning and courtship signals In a final step, we deduce the statistics of natural electrosensory stimuli resulting from the observed communication behaviors and relate it to the known physiological properties of electrosensory neurons. Superposition of a fish's EOD with that of a nearby fish results in a periodic amplitude modulation, a so-called beat. Both frequency and amplitude of the beat provide a crucial signal background for the neural encoding of communication signals (Marsat et al., 2012). The beat frequency is given by the difference between the two EODfs and the beat amplitude equals the EOD amplitude of the nearby fish at the position of the receiving fish (Fotowat et al., 2013) (Fig. 8 A). The amplitude modulations are encoded by

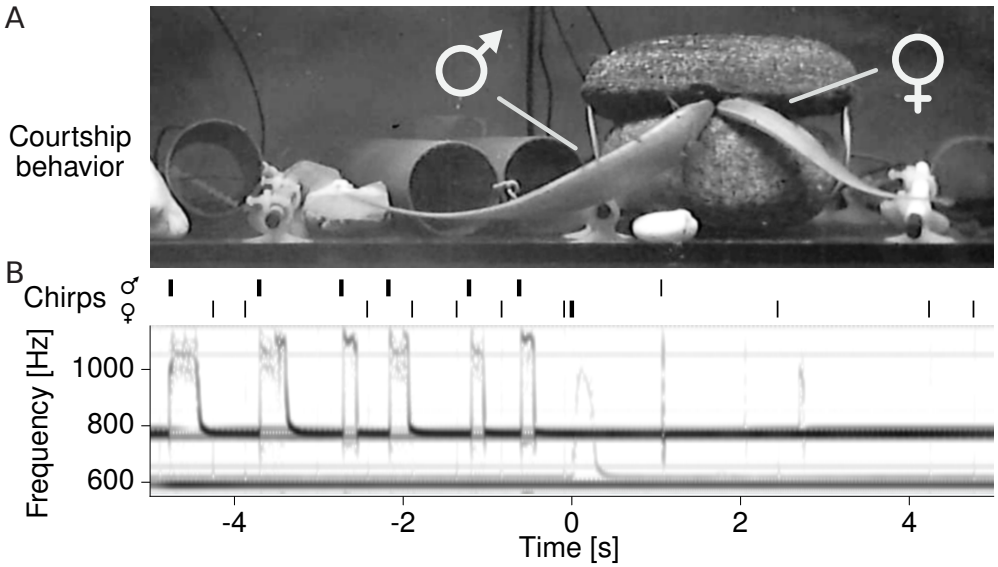

Figure 7: Synchronizing role of the female long chirp in spawning. A) Simultaneous video (snapshot of movie S 7) and B) voltage recordings (spectrogram) of *A. leptorhynchus* in the laboratory demonstrate the synchronizing function of the female long chirp (at time zero; trace with EOD$f = 608$ Hz baseline frequency) in spawning. In contrast to *A. rostratus,* male *A. leptorhynchus* generate an additional, long chirp type before spawning (top trace with EOD$f = 768$ Hz baseline frequency). Chirp onset times of the male and the female are marked by vertical bars above the spectrogram. Thick and thin lines indicate long and short duration chirps, respectively.

tuberous electroreceptors (P-units) distributed over the fish's skin (Bastian, 1981a; Carr et al., 1982; Nelson et al., 1997; Benda et al., 2006; Walz et al., 2014).

We estimated the population activity of P-unit afferents in *A. leptorhynchus* from the standard deviation of the summed nerve activity, which is known to closely match the tuning properties of single nerve fibers (Benda et al., 2006; Walz et al., 2014). The P-unit population response quickly dropped to low signal-to-noise ratios (Cohen's $d < 1$) at amplitudes corresponding to inter-fish distances larger than about 30 cm at 60 Hz beat frequency (Fig. 8 B). P-unit afferents are also tuned to beat frequency and are most sensitive around 60 Hz (Bastian, 1981a; Walz et al., 2014) (Fig. 8 E), covering well the beat frequencies arising from same-sex interactions (Fig. 8 H). Remarkably, all courtship chirping occurred at much higher beat frequencies (205–415 Hz, Fig. 8 G and Fig. 4 B). Even though the beat amplitudes during these interactions are large at the observed small distances of less than 32 cm (Fig. 8 C), such high-frequency stimuli evoke only weak P-unit activity ($d < 0.83$ at an amplitude corresponding to the closest measured distance for 260 Hz beat frequency). High beat frequencies are not a rare occurrence as the probability distribution of 406 beat frequencies measured from encounters in 5 nights show (Fig. 8 F), demonstrating a clear frequency mismatch between an important group of behaviorally relevant sensory signals and electroreceptor

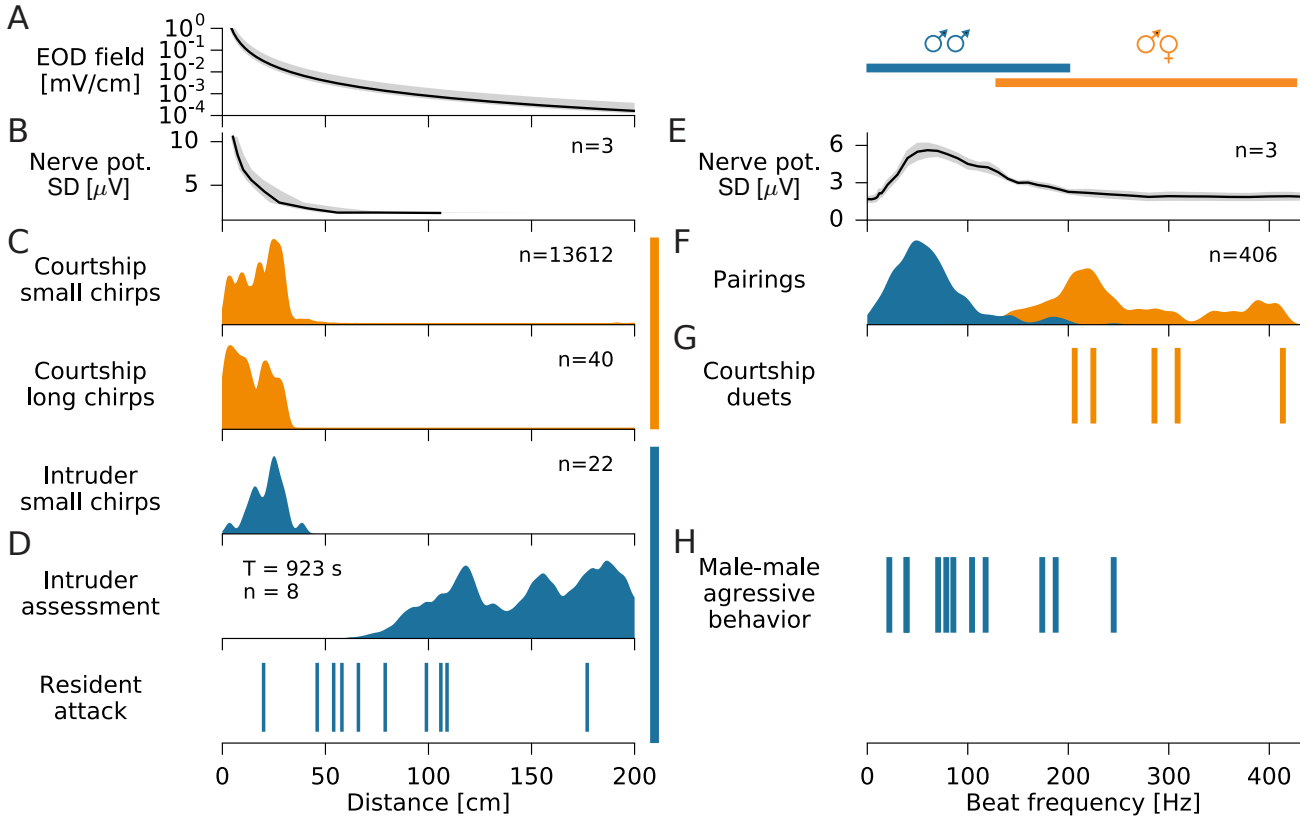

Figure 8: Non-optimal encoding of behaviorally relevant natural stimuli. A) Maximum electric field strength as a function of distance from the emitting fish (median with total range). B) Activity of the electroreceptor afferent population rapidly declines with distance between two fish (beat frequency 60 Hz). C) Small and long chirps in both courtship and aggression contexts are emitted consistently at distances below 32 cm. D) Intruder assessment and initiation of attacks by residents occur at much larger distances (movie S 6). E) Tuning of electroreceptor afferent activity to beat frequency. F) Distribution of beat frequencies of all *A. rostratus* appearing simultaneously in the electrode array. blue: male-male, orange: male-female ($n = 406$ pairings). G) Courtship behaviors occurred at beat frequencies in the range of 205–415 Hz, far from the receptors' best frequency. H) Aggressive interactions between males occurred at beat frequencies below 245 Hz, better matching the tuning of the electroreceptor afferents.

tuning.

Communication at long distances In contrast, two behaviors involving intruding males occurred within the P-units' best-frequency range (Fig. 8 H), but at large distances (Fig. 8 D): (i) Intruding males initially often lingered at distances larger than 70 cm from the courting dyad (8 of 16 scenes, median duration 58.5 s; e.g., Fig. 2 A, movie S 5), consistent with assessment behavior (Arnott and Elwood, 2008). (ii) The distances at which resident males started to attack intruders ranged from 20 cm to 177 cm (81 ± 44 cm, $n = 10$, Fig. 2 B, movie S 6). At the largest observed attack distance of 177 cm, the electric field strength was estimated to be maximally 0.34 μV/cm (assuming the fish were oriented optimally) — a value close to minimum behavioral threshold values of about 0.1 μV/cm measured in the laboratory at the fish's best frequency (Knudsen, 1974; Bullock et al., 1972). Both situations, opponent assessment and decision to attack, therefore evoke weak activity of P-units close to the fish's perception threshold.

Discussion

We recorded movement and electrocommunication signals in a wild population of the weakly-electric fish, *Apteronotus rostratus*, in their natural neotropical habitat by means of a submerged array of electrodes. A stereotyped pattern of interactive chirping climaxed in a special long chirp emitted by the female that we identified in a breeding experiment as a synchronizing signal for spawning. This electrocommunication behavior was characterized by echo responses by the male on a 100 ms time-scale and concurrent increases in chirp rate in dyads on a tens-of-seconds time-scale. The frequencies associated with courtship signals, however, were much higher than the optimal tuning range of electroreceptor afferents. As a consequence, courtship signals barely activate the electrosensory system. On the other hand, signals arising in some male-male aggressive interactions match the tuning of electroreceptors, but are nevertheless weak because of the large distance between the fish. These findings demonstrate that many important sensory signals are clearly not optimally encoded by peripheral electrosensory neurons. The observed behaviors indicate, however, that higher brain areas must be able to extract the relevant information reliably.

Communication in the wild and in the laboratory Animal communication is defined as the transfer of information by a signal generated by the sender that affects the behavior of the receiving animal (Wilson, 1975). Our observations of male echo responses to female chirps occurring reliably within a few tens of milliseconds (Figs. 6 A, C), precisely timed chirp doublets in response to female long chirps (Figs. 3), immediate behavioral reactions of males to female long chirps (Fig. 7, movie S 7), and females slowly raising their chirp rate in response to male chirp-

ing (Fig. 5) clearly qualify chirps as communication signals in natural conditions. Laboratory studies have found slower echo responses on timescales of a few seconds exclusively between males (Hupé and Lewis, 2008; Zupanc et al., 2006; Salgado and Zupanc, 2011) and inhibiting effects of small chirps on attack behavior (Walz et al., 2013). Such a submissive function of male-to-male chirping is supported by our observations of a few chirps emitted by an intruder while being driven away by a dominant resident male. The number of chirps generated in these aggressive contexts is, however, much lower (1 to 10, median 3, chirps in 5 of 9 pairings, Fig. 4) compared to encounters staged in the laboratory (about 125 chirps per 5 min trial, Hupé and Lewis, 2008). Our field data do not support a function of chirps as signals of aggression and dominance (Triefenbach and Zakon, 2008). These differences may be due to the specific conditions under which the laboratory experiments were conducted.

In so-called "chirp chamber" experiments small chirps were predominantly generated by males at beat frequencies well below about 150 Hz, corresponding to same-sex interactions (Engler and Zupanc, 2001). On the contrary, in our observations on *A. rostratus* in the field and reproductive *A. leptorhynchus* in the laboratory, both male and female fish were almost exclusively chirping in male-female contexts at beat frequencies above about 200 Hz (Fig. 4 B). Also, the maximum small-chirp rates during courtship exceeded maximum rates reported from laboratory observations (Engler and Zupanc, 2001; Hupé and Lewis, 2008). Last but not least, the total number of chirps we recorded in two nights of courtship activity exceeded the so far published number of chirps recorded under artificial laboratory conditions by an order of magnitude (see Smith (2013) for a review). This large number of chirps allowed us to draw firm conclusions about the function of chirping.

Duetting during courtship Previous laboratory studies already suggested a function of the EOD and its modulations in courtship in *A. rostratus* (Hagedorn and Heiligenberg, 1985; Hagedorn, 1988) and in the synchronization of spawning and external fertilization in the pulse-type gymnotiform *Brachyhypopomus pinnicaudatus* (Silva et al., 2008). Our results provide strong evidence that female long chirps are an exclusive communication signal for the synchronization of egg spawning and sperm release: (i) The female long chirp was the central part of a highly stereotyped duet-like communication pattern between a male and female fish (Fig. 3 and Fig. 5). Multimodal signals synchronizing egg and sperm release have been observed in other aquatic animals (Lobel, 1992; Ladich, 2007). (ii) Fertilized eggs were found at the locations of male-female interaction, and only when the female had produced long chirps in the preceding night. (iii) The period immediately before the female long chirp was characterized by extensive chirp production by the male (Fig. 5), consistent with male courting behavior (Bradbury and Vehrencamp, 2011). (iv) Video sequences triggered on female long chirps clearly demonstrated the special role of the female long chirp (Fig. 7, movie S 7). We hypothesize that the synchronization of external fertilization via

extensive electrocommunication gives females good control over who they reproduce with.

The males appear to compete for access to females. This and the observed serial consortship suggest a scramble competition mating system as it is common for animals living in a three-dimensional environment, e.g., fish and birds (Bradbury and Vehrencamp, 2011).

Non-optimal encoding of behaviorally relevant signals The distribution of beat frequencies (Fig. 8 F) and the obvious relevance of high frequencies for male-female communication is not reflected by the very low and flat tuning curve of the receptors in the high frequency range (Fig. 8 E, (Walz et al., 2014)), indicating a non-optimal neural representation of these signals. The profound mismatch between the tuning of receptor neurons and the high beat frequencies occurring during courtship is unexpected given the many examples of optimally encoded courtship signals in other sensory systems (Rieke et al., 1995; Machens et al., 2005; Kostarakos et al., 2009; Schrode and Bee, 2015). This mismatch is also unexpected from the perspective of the design of animal communication systems (Bradbury and Vehrencamp, 2011) and points to selective forces beyond the need for the male to provide strong stimulation to the female sensory system. In addition to the substantial metabolic cost of the active electrosensory system incurred by continuously generating an EOD (Salazar et al., 2013; Markham et al., 2016), this mismatch potentially also imposes a computational cost on the sensory system. The high beat-frequencies in male-female interactions are a consequence of a sexual dimorphism in EODf where males have higher frequencies (here 907 ± 77 Hz, $n = 10$) than females (here 640 ± 23 Hz, $n = 5$). In the genus *Apteronotus* the presence, magnitude, and direction of an EODf dimorphism varies considerably across species and thus is evolutionary labile (Smith, 2013). This points to very specific and subtle selection pressures generating EODf dimorphisms that offset the reduced sensitivity for mates.

Encoding of non-optimal high-frequency stimuli Male echo responses to female chirps occurring reliably within a few tens of milliseconds (Figs. 6 A, C), precisely timed chirp doublets (Figs. 3), and long-range assessment and attacks (Fig. 8 D) demonstrate that the respective electrocommunication signals are successfully and robustly evaluated by the electrosensory system, despite the weak receptor activation that these interactions generate. A similar sensitivity of the electrosensory system has been shown in the context of prey detection where stimuli are low in frequency (< 25 Hz) and small in amplitude (Nelson and MacIver, 1999).

How could the high-frequency courtship signals be encoded and processed by the electrosensory system? Gymnotiform weakly electric fish have three types of electroreceptor cells: (i) Ampullary receptors are tuned to low-frequency (< 50 Hz) external electric fields and therefore do not encode the EOD with its EODf of more than about 600 Hz (Grewe et al., 2017) and chirps in *Apteronotus* that have no low-frequency component (Metzner and

Heiligenberg, 1991; Stöckl et al., 2014). (ii) In *Eigenmannia* T-unit tuberous receptors help to disambiguate the sign of the beat in the context of the jamming avoidance response (JAR) below about 15 Hz (Bullock et al., 1972; Rose and Heiligenberg, 1985). However, T-units are rare in *Apteronotus* (Maler et al., 1981; Heiligenberg and Dye, 1982). (iii) P-units, the second and dominant type of tuberous receptors (Carr et al., 1982), encode amplitude modulations of the fish's EOD in their firing rate (Scheich et al., 1973; Bastian, 1981a; Nelson et al., 1997; Benda et al., 2005; Walz et al., 2014). Thus, P-units are the only type of electroreceptors that are able to encode the wide range of amplitude modulations generated by beats and chirps in *Apteronotus*.

The tuning of P-units to beat frequencies has been characterized up to 300 Hz by single-unit recordings in both *A. albifrons* and *A. leptorhynchus* (Bastian, 1981a; Nelson et al., 1997; Benda et al., 2006; Walz et al., 2014). All studies agree that the average P-unit response is strongest at beat frequencies of about 30 to 130 Hz and declines almost back to baseline levels at 300 Hz in accordance with our measurements (Fig. 8 E). However, P-units are heterogeneous in their baseline activity (Gussin et al., 2007; Savard et al., 2011; Grewe et al., 2017) and P-units with high baseline rates might show frequency tuning that extends to higher frequencies than the average tuning of the population (Knight, 1972). This is supported by noticeable stimulus-response coherences that have been measured with narrowband noise stimuli up to 400 Hz (Savard et al., 2011). Most of these studies used rather strong beat amplitudes of more than 10 % of the EOD amplitude. We observed chirp interactions at distances up to 32 cm, corresponding to beat amplitudes from 100 % down to about 1 % of the EOD amplitude. Smaller beat amplitudes result in down-scaled frequency tuning curves (Bastian, 1981a; Benda et al., 2006). In particular, for amplitudes below 10 %, responses to beat frequencies larger than 200 Hz are close to baseline activity (Benda et al., 2006).

Chirp encoding can be understood based on the frequency tuning of P-units (Walz et al., 2014). A chirp transiently increases the beat frequency. The response to the chirp differs only as much from the response to the background beat as the frequency response to the chirp differs from the one to the beat. Therefore, we expect chirp coding to be additionally impaired by the low slope of the P-unit's frequency tuning curve at high beat frequencies.

Decoding The robust behavioral responses suggest that the weak, non-optimal activation of electroreceptor neurons is compensated for at later processing stages. The compensating mechanisms likely involve synchrony detection (Middleton et al., 2009; Grewe et al., 2017), averaging (Maler, 2009b; Jung et al., 2016), and feedback connections from higher brain areas, including the telencephalon (Giassi et al., 2012; Krahe and Maler, 2014), that modulate the first stage of electrosensory processing in the hindbrain (Bastian, 1986). P-units converge onto pyramidal cells in the electrosensory lateral line lobe (ELL) (Heiligenberg and Dye, 1982; Bastian, 1981b; Maler,

2009a). The pyramidal cells processing communication signals (Metzner and Juranek, 1997; Krahe et al., 2008; Vonderschen and Chacron, 2011; Marsat et al., 2012) integrate over 1000 P-units each (Maler, 2009a), their tuning curves peak at frequencies similar to or lower than those of P-units (Bastian, 1981b), and their stimulus-response coherences peak well below 100 Hz, but have only been measured up to 120 Hz (Chacron et al., 2003; Chacron, 2006; Krahe et al., 2008). Coding of small chirps by pyramidal cells in the ELL has so far only been studied at beat frequencies below 60 Hz (Vonderschen and Chacron, 2011; Marsat et al., 2012). Thus, most electrophysiological recordings from the electrosensory system have been biased to low beat frequencies and strong stimulus amplitudes evoking obvious neuronal responses, but ignoring the behaviorally most relevant stimuli (Olshausen and Field, 2005).

Hormonal influences Depending on the state of the animal, electrosensory tuning may be modified, e.g., by hormones and/or neuromodulators. Steroids are known to modulate EODf and tuning of P-units to EODf (Meyer and Zakon, 1982; Meyer et al., 1987; Dunlap et al., 1998). Serotonin is a neuromodulator that is released in the ELL in response to communication signals (Fotowat et al., 2016) and potentially enhances activity levels in ELL (Deemyad et al., 2013). Activation of muscarinic receptors by acetylcholine has been shown to improve low-frequency coding of pyramidal cells (Ellis et al., 2007). Whether and how hormones or neuromodulators influence coding of high-frequency beats is not known yet.

Conclusion Our observations regarding sex-specificity, numbers, and functions of chirps differ substantially from laboratory studies. Limited space and artificial settings may have biased interactions towards aggressive behaviors. In the wild, these aggressive encounters were rare and were accompanied by only little or no chirping. In contrast, courtship scenes stood out as highly structured and long-lasting sequences of high-frequency chirping. We have shown that similar courtship behavior can be reproduced in the laboratory by giving the fish enough time to interact — several month instead of minutes or hours.

The fish robustly responded to courtship signals although courtship signals activate P-unit electroreceptors only weakly at the tail of their tuning curve. The extent of this mismatch in frequency tuning was unexpected given previous, mainly laboratory-based findings (Walz et al., 2013). For the first time we observed long-distance interactions between competing males that also emphasize the ability of the electrosensory system to process relevant signals close to threshold reliably. Our field data thus identify important — but so far neglected — stimulus regimes of the electrosensory system and provide further evidence for the existence of sensitive neural mechanisms for the detection of such difficult sensory signals (Gao and Ganguli, 2015).

The analysis of field data from the natural environments a specific species evolved in could point to behav-

iorally relevant sensory scenes that are otherwise neglected because they do not obviously excite sensory neurons (Olshausen and Field, 2005). Here, this is exemplified for weakly-electric fish. For other organisms and sensory sytems field data may as well reveal unexpected sensory scenes. Such difficult and complex signals that nevertheless are behaviorally relevant open new windows for investigating the real challenges faced and solved by sensory systems.

Materials and methods

Field site

The field site is located in the Tuira River basin, Province of Darin, Republic of Panam (fig. S 1 A), at Quebrada La Hoya, a narrow and slow-flowing creek supplying the Chucunaque River. Data were recorded about 2 km from the Ember community of Pea Bijagual and about 5 km upstream of the stream's mouth (8°15′13.50″N, 77°42′49.40″W). The water of the creek is clear, but becomes turbid for several hours after heavy rainfall. The creek flows through a moist secondary tropical lowland forest, which, according to local residents, gets partially flooded on a regular basis during the wet season (May – November). The water levels of the creek typically range from 20 – 130 cm at different locations, but can rise temporarily to over 200 cm after heavy rainfall. At our recording site (fig. S 1 B), the water level ranged from 20 – 70 cm. The banks of the creek are typically steep and excavated, consisting mostly of root masses of large trees. The water temperature varied between 25 and 27 °Con a daily basis and water conductivity was stable at 150 – 160 µS/cm. At this field site we recorded four species of weakly electric fish, the pulse-type fish *Brachyhypopomus occidentalis* (˜30 – 100 Hz pulses per second), the wave-type species *Sternopygus dariensis* (EODf at ˜40 – 220 Hz), *Eigenmannia humboldtii* (˜200 – 600 Hz), and *Apteronotus rostratus* (˜600 – 1100 Hz). We here focused exclusively on *A. rostratus*, a member of the *A. leptorhynchus* species group (brown ghost knifefish (de Santana and Vari, 2013)) and its intraspecies interactions.

Field monitoring system

Our recording system (Fig. 1 C, fig. S 1 B) consisted of a custom-built 64-channel electrode and amplifier system (npi electronics GmbH, Tamm, Germany) running on 12 V car batteries. Electrodes were low-noise headstages encased in epoxy resin (1× gain, 10 × 5 × 5 mm). Signals detected by the headstages were fed into the main amplifier (100× gain, 1st order high-pass filter 100 Hz, low-pass 10 kHz) and digitized with 20 kHz per channel with 16-bit amplitude resolution using a custom-built low-power-consumption computer with two digital-analog converter cards (PCI-6259, National Instruments, Austin, Texas, USA). Recordings were controlled with custom

software written in C++ (https://github.com/bendalab/fishgrid) that also saved data to hard disk for offline analysis (exceeding 400 GB of uncompressed data per day). Raw signals and power spectra were monitored online to ensure the quality of the recordings. We used a minimum of 54 electrodes, arranged in an 9×6 array covering an area of 240×150 cm (30 cm spacing). The electrodes were mounted on a rigid frame (thermoplast 4×4 cm profiles, 60 % polyamid, 40% fiberglass; Technoform Kunststoffprofile GmbH, Lohfelden, Germany), which was submerged into the stream and fixed in height 30 cm below the water level. Care was taken to position part of the electrode array below the undercut banks of the stream in order to capture the EODs of fish hiding in the root masses. The recording area covered about half of the width of the stream and the hiding places of several electric fish. The maximum uninterrupted recording time was limited to 14 hours, determined by the capacity of the car batteries (2×70 Ah) and the power consumption of the computer (22 W) and amplifier system (25 W).

Data analysis

All data analysis was performed in Python 2.7 (www.python.org, https://www.scipy.org/). Scripts and raw data (Panama field data: 2.0 TB, Berlin breeding experiment: 3.7 TB of EOD recordings and 11.4 TB video files) are available on request, some of the core algorithms are accessible at https://github.com/bendalab/thunderfish. Summary data are expressed as means $\pm$ standard deviation, unless indicated otherwise.

Spectrograms Spectrograms in Fig. 3 and Fig. 7 B were calculated from data sampled at 20 kHz in windows of 1024 and 2048 data points , corresponding to 51.2 ms and 102.4 ms, respectively, applying a Blackman window function. Sequential windows were shifted by 50 data points (2.5 ms). The resulting spectrograms were interpolated in the frequency dimension for visual purposes using a resolution of 2 Hz and were then thresholded to remove low power background.

Fish identification and tracking Our EOD tracking system is optimized for identifying and tracking individual wave-type electric fish, to estimate the fish's positions, and to detect communication signals. The signals of pulse-type electric fish were detected, but remain unprocessed for now. First, information about electric fish presence, EOD frequency (EODf), and approximate position were extracted. Each electrode signal was analyzed separately in sequential overlapping windows (1.22 s width, 85 % overlap). For each window the power spectral density was calculated (8192 FFT data points, 5 sub-windows, 50% overlap) and spectral peaks above a given threshold were detected. Individual fish were extracted from the list of peak frequencies, based on the harmonic structure of wave-type EODs. For each analysis window, EOD detections from all electrodes were matched and consolidated. Finally, fish detections in successive time windows were matched, combined, and stored for further analysis.

Position estimation Once the presence of an electric fish was established, the fish's position was estimated and chirps were detected. For each fish, the signals of all electrodes were bandpass-filtered (forward-backward butterworth filter, 3rd order, 5× multipass, ±7 Hz width) at the fish's EODf. Then the envelope was computed from the resulting filtered signal using a root-mean-square filter (10 EOD cycles width). Each 40 ms the fish position $\vec{x}$ was estimated from the four electrodes i with the largest envelope amplitudes A_i at position $\vec{e}_i$ as a weighted spatial average

$$\vec{x} = \frac{\sum_{i=1}^{n=4} \sqrt{A_i} \cdot \vec{e}_i}{\sum_{i=1}^{n=4} \sqrt{A_i}}$$

(movie S 4). If fewer than two electrodes with EOD amplitudes larger than 15 µV were available, the position estimate was omitted. Although this estimate does not relate to the underlying physics of the electric field, it proved to be the most robust against interference by electrical noise (Hopkins, 1973) and fish moving close to the edges of the electrode array, as verified with both experiments and simulations. For the electrode configuration used, the weighted spatial average yielded a precision of 4.2±2.6 cm on level with the electrode array and 6.2±3.8 cm at a vertical distance of 15 cm as computed by extensive simulations. Finally, the position estimates were filtered with a running average filter of 200 ms width to yield a smoother trace of movements. For pulse-type electric fish an EOD-based method for tracking electric fish position in shallow water in a laboratory setup has been published recently, yielding slightly better precision with a physically more realistic lookup-table-based approach (Jun et al., 2013).

Chirp detection and analysis For each fish the electrode voltage traces were bandpass-filtered (forward-backward butterworth filter, 3rd order, 5× multipass, ±7 Hz width) at the fish's EODf and at 10 Hz above the EODf. For each passband the signal envelope was estimated using a root-mean-square filter over 10 EOD cycles. Rapid positive EOD frequency excursions cause the signal envelope at the fish's baseline frequency to drop and in the passband above the fish's EODf to increase in synchrony with the frequency excursion. If events were detected synchronously in both passbands on more than two electrodes, and exceeded a preset amplitude threshold, they were accepted as communication signals.

Communication signals with a single peak in the upper passband were detected as small chirps. Signals of up to 600 ms duration and two peaks in the upper passband, marking the beginning and the end of the longer frequency modulation, were detected as long chirps. All chirps in this study were verified manually. However, it is likely that some chirps were missed, since detection thresholds were set such that the number of false positives was very low.

Interchirp-interval probability densities were generated for pairs of fish and only for the time period in which both fish were producing chirps. Kernel density histograms of interchirp intervals (Fig. S 2) were computed with a

Gaussian kernel with a standard deviation of 20 ms.

Rates of small chirps before and after female long chirps (Fig. 5 A, C) were calculated by convolving the chirp times with a Gaussian kernel ($\sigma = 0.5$ s) separately for each episode and subsequently calculating the means and standard deviations.

For quantifying the echo response (Fig. 6) we computed the cross-correlogram

$$r(\tau) = \frac{1}{n_a} \sum_{j=1}^{n_a} \sum_{i=1}^{n_b} g(\tau - (t_{b,i} - t_{a,j}))$$

with the n_a chirp times $t_{a,j}$ of fish a and the n_b chirp times $t_{b,i}$ of fish b using a Gaussian kernel $g(t)$ with a standard deviation of 20 ms. To estimate its confidence intervals, we repeatedly resampled the original dataset (2000 times jackknife bootstrapping; random sampling with replacement), calculated the cross-correlogram as described above and determined the 2.5 and 97.5 % percentiles. To create the cross-correlograms of independent chirps, we repeatedly (2000 times) calculated the cross-correlograms on chirps jittered in time by adding a random number drawn from a Gaussian distribution with a standard deviation of 500 ms and determined the mean and the 2.5 and 97.5 % percentiles. Deviations of the observed cross-correlogram beyond the confidence interval of the cross-correlogram of jittered chirp times are significant on a 5 % level, and are indicative of an echo response. Reasonable numbers of chirps for computing meaningful cross-correlograms (more than several hundreds of chirps) were available in five pairs of fish.

Beat frequencies and spatial distances The distance between two fish at the time of each chirp (Fig. 8 C) was determined from the estimated fish positions. Because position estimates were not always available for each time point we allowed for a tolerance of maximally two seconds around the chirp for retrieving the position estimate. The positions were compiled into kernel density histograms that were normalized to their maximal value. The Gaussian kernel had a standard deviation of 1 cm for courtship small chirps, and 2 cm for courtship long chirps as well as intruder small chirps. Males ($n = 8$) intruding on a courting dyad initially lingered at some distance from the dyad before either approaching the dyad further or being chased away by the courting resident male. Distances between the intruding male and the courting male during this assessment behavior (Fig. 8 D, top) were measured every 40 ms beginning with the appearance of the intruding fish until the eventual approach or attack. These distances, collected from a total assessment time of 923 s, were summarized in a kernel density histogram with Gaussian kernels with a standard deviation of 2 cm.

When a male intruded on a courting dyad it was directly attacked by the resident male. In that process courtship was always interrupted and eventually one of the males withdrew. In some cases a few chirps were emitted by the

retreating male. The winning male always approached and courted the female. The attack distances between two males (Fig. 8 D, bottom) were determined at the moment a resident male initiated its movement toward an intruding male. This moment was clearly identifiable as the onset of a linear movement of the resident male towards the intruder from plots showing the position of the fish as a function of time.

The distribution of beat frequencies generated by fish present in the electrode array at the same time (Fig. 8 F) was calculated from all available recordings during the breeding season. The average frequency difference of each pair of fish simultaneously detected in the recordings was compiled into a kernel density histogram with a Gaussian kernel with a standard deviation of 10 Hz. Similarly, for courtship and aggressive behavior (Fig. 8 G, H) the mean frequency differences were extracted for the duration of these interactions.

Electric fields For an estimation of EOD amplitude as a function of distance, histograms of envelope amplitudes from all electrodes of the array were computed as a function of distance between the electrodes and the estimated fish position. For each distance bin in the range of 20 – 100 cm the upper 95 % percentile of the histogram was determined and a power law was fitted to these data points. Gymnotiform electroreceptors measure the electric field, i.e., the first spatial derivative of the EOD amplitudes as shown in Fig. 8 A.

Breeding monitoring setup

In the laboratory breeding study, we used the brown ghost knifefish *Apteronotus leptorhynchus*, a close relative of *A. rostratus* (de Santana and Vari, 2013). *Apteronotus leptorhynchus* is an established model organism in neuroscience and readily available from aquarium suppliers. The two species share many similarities. (i) Most chirps produced by both species are "small chirps" that in *A. leptorhynchus* have been classified as type-2 chirps (Engler and Zupanc, 2001). (ii) Females of both species additionally generate small proportions of "long chirps", similar to the type-4 chirps classified for *A. leptorhynchus* males. (iii) Both species show the same sexual dimorphism in EODf.

The laboratory setup for breeding *A. leptorhynchus* consisted of a holding tank ($100 \times 45 \times 60$ cm) placed in a darkened room and equipped with bubble filters and PVC tubes provided for shelter. Heating was supplied via room temperature, which kept water temperature between 21 and 30 °C. The light/dark cycle was set to 12/12 hours. Several pieces of rock were placed in the center of the tank as spawning substrate. EOD signals were recorded differentially using four pairs of graphite electrodes. Two electrode pairs were placed on each side of the spawning substrate. The signals were amplified and analog filtered using a custom-built amplifier (100× gain, 100 Hz high-pass, 10 kHz low-pass; npi electronics GmbH, Tamm, Germany), digitized at 20 kHz with 16 bit (PCI-6229, National Instruments, Austin, Texas, USA), and saved to hard disk for offline analysis. The electrode pairs

were positioned orthogonally to each other, thereby allowing for robust recordings of EODs independent of fish orientation. The tank was illuminated at night with a dozen infrared LED spotlights (850 nm, 6W, ABUS TV6700) and monitored continuously (movie S 7) with two infrared-sensitive high-resolution video cameras (Logitech HD webcam C310, IR filter removed manually). The cameras were controlled with custom written software (https://github.com/bendalab/videoRecorder) and a timestamp for each frame was saved for later synchronization of the cameras and EOD recordings. Six fish of *A. leptorhynchus* (three male, three female; imported from the Ro Meta region, Colombia) were kept in a tank for over a year before being transferred to the recording tank. First, fish were monitored for about a month without external interference. We then induced breeding conditions (Kirschbaum and Schugardt, 2002) by slowly lowering water conductivity from 830 µS/cm to about 100 µS/cm over the course of three months by diluting continuously the tank water with deionized water. The tank was monitored regularly for the occurrence of spawned eggs.

Electrophysiology

For *in vivo* recordings fish were anesthetized with MS-222 (120 mg/l; PharmaQ, Fordingbridge, UK; buffered to pH 7 with sodium bicarbonate) and a small part of the skin was removed to expose the anterior part of the lateral line nerve that contains only electroreceptor afferent fibers innervating electroreceptors on the fish's trunk (Maler et al., 1974). The margin of the wound was treated with the local anesthetic Lidocaine (2%; bela-pharm, Vechta, Germany). Then the fish was immobilized by intramuscular injection of Tubocurarine (Sigma-Aldrich, Steinheim, Germany; 25 – 50 µl of 5 mg/ml solution), placed in a tank, and respired by a constant flow of water through its mouth. The water in the experimental tank ($47 \times 42 \times 12$ cm) was from the fish's home tank with a conductivity of about 300 µS/cm and kept at 28 °C. All experimental protocols were approved by the local district animal care committee and complied with federal and state laws of Germany (file no. ZP 1/13) and Canada.

Population activity in whole-nerve recordings was measured using a pair of hook electrodes of chlorided silver wire. Signals were differentially amplified (gain 10 000) and band-pass filtered (3 to 3 000 Hz passband, DPA2-FX; npi electronics), digitized (20 kHz sampling rate, 16-bit, NI PCI-6229; National Instruments), and recorded with RELACS (www.relacs.net) using efield and efish plugins. The strong EOD artifact in this kind of recording was eliminated before further analysis by applying a running average of the size of one EOD period (Benda et al., 2006). The resulting signal roughly followed the amplitude modulation of the EOD and we quantified its amplitude by taking its standard deviation. The nerve recordings closely resemble the properties of P-unit responses obtained from single and dual-unit recordings (Benda et al., 2006; Walz et al., 2014). Note, however, that P-units might still respond in subtle ways to a stimulus even though the nerve recording is already down at baseline level, because

of additional noise sources in this kind of recording. Signal-to-noise ratios were simply computed as Cohen's d between the responses and baseline activity.

Electric sine-wave stimuli with frequencies ranging from $\Delta f = -460$ to $+460$ Hz in steps of 2 Hz ($|\Delta f| \leq 20$ Hz), 10 Hz ($|\Delta f| \leq 200$ Hz), and 20 Hz ($|\Delta f| > 200$ Hz) relative to the fish's EODf were applied through a pair of stimulation electrodes (carbon rods, 30 cm long, 8 mm diameter) placed on either side of the fish. Stimuli were computer-generated and passed to the stimulation electrodes after being attenuated to the right amplitude (0.05, 0.1, 0.2, 0.5, 1.0, 2.5, 5.0, 10.0, 20.0, 40.0 % of the fish's EOD amplitude estimated with a pair of electrodes separated by 1 cm perpendicular to the side of the fish) and isolated from ground (Attenuator: ATN-01M; Isolator: ISO-02V; npi electronics). For more details see Benda et al. (2006); Walz et al. (2014).

Acknowledgment

Supported by the BMBF Bernstein Award Computational Neuroscience 01GQ0802 to J.B., a Discovery Grant from the Natural Sciences and Engineering Research Council of Canada to RK, and a Short Time Fellowship to J.H. from the Smithonian Tropical Research Institute. We thank Hans Reiner Polder and Jrgen Planck from npi electronic GmbH for designing the amplifier, Sophie Picq, Diana Sharpe, Luis de Len Reyna, Rigoberto Gonzlez, Eldredge Bermingham, the staff from the Smithsonian Tropical Research Institute, and the Ember community of Pea Bijagual for their logistical support, Fabian Sinz for advice on the analysis, and Ulrich Schnitzler and Janez Presern for comments on the manuscript.

Competing interests

Authors declare no conflicts of interest.

References

Arnott G, Elwood RW (2008) Information gathering and decision making about resource value in animal contests. Anim Behav 76:529–542.

Bastian J (1981a) Electrolocation I. How electroreceptors of *Apteronotus albifrons* code for moving objects and other electrical stimuli. J Comp Physiol 144:465–479.

Bastian J (1981b) Electrolocation II. The effects of moving objects and other electrical stimuli on the activities of two categories of posterior lateral line lobe cells in *Apteronotus albifrons*. J Comp Physiol 144:481–494.

Bastian J (1986) Gain control in the electrosensory system mediated by descending inputs to the electrosensory lateral line lobe. J Neurosci 6:553–562.

Benda J, Longtin A, Maler L (2005) Spike-frequency adaptation separates transient communication signals from background oscillations. J Neurosci 25:2312–2321.

Benda J, Longtin A, Maler L (2006) A synchronization-desynchronization code for natural communication signals. Neuron 52:347–358.

Betsch BY, Einhäuser W, Körding KP, König P (2004) The world from a cat's perspective — statistics of natural videos. Biol Cybern 90:41–50.

Bradbury JW, Vehrencamp SL (2011) Principles of animal communication. Sunderland: Sinauer, 2nd edition.

Bullock TH, Hamstra RH, Scheich H (1972) The jamming avoidance response of high frequency electric fish. II. Quantitative aspects. J Comp Physiol 77:23–48.

Carr CE, Maler L, Sas E (1982) Peripheral organization and central projections of the electrosensory nerves in gymnotiform fish. J Comp Neurol 211:139–153.

Chacron MJ (2006) Nonlinear information processing in a model sensory system. J Neurophysiol 95:2933–2946.

Chacron MJ, Doiron B, Maler L, Longtin A, Bastian J (2003) Non-classical receptive field mediates switch in a sensory neuron's frequency tuning. Nature 423:77–81.

Clemens J, Ronacher B (2013) Feature extraction and integration underlying perceptual decision making during courtship behavior. J Neurosci 33:12136–12145.

Deemyad T, Metzen MG, Pan Y, Chacron MJ (2013) Serotonin selectively enhances perception and sensory neural response to stimuli generated by same sex conspecifics. PNAS 110:19609–19614.

Dunlap KD, Thomas P, Zakon HH (1998) Diversity of sexual dimorphism in electrocommunication signals and its androgen regulation in a genus of electric fish, *Apteronotus*. J Comp Physiol A 183:77–86.

Ellis LD, Krahe R, Bourque CW, Dunn RJ, Chacron MJ (2007) Muscarinic receptors control frequency tuning through the downregulation of an A-type potassium current. J Neurophysiol 98:1526–1537.

Engler G, Zupanc GK (2001) Differential production of chirping behavior evoked by electrical stimulation of the weakly electric fish, *Apteronotus leptorhynchus*. J Comp Physiol A 187:747–756.

Fotowat H, , Harvey-Girard E, Cheer JF, Krahe R, Maler L (2016) Subsecond sensory modulation of serotonin levels in a primary sensory area and its relation to ongoing communication behavior in a weakly electric fish. eNeuro 3:e0115–16.2016 1–12.

Fotowat H, Harrison RR, Krahe R (2013) Statistics of the electrosensory input in the freely swimming weakly electric fish *Apteronotus leptorhynchus*. J Neurosci 33:13758–13772.

Fugère V, Ortega H, Krahe R (2011) Electrical signalling of dominance in a wild population of electric fish. Biol Lett 7:197–200.

Gao P, Ganguli S (2015) On simplicity and complexity in the brave new world of large-scale neuroscience. Curr Opin Neurobiol 334:666–670.

Giassi ACC, Duarte TT, Ellis W, Maler L (2012) Organization of the gymnotiform fish pallium in relation to learning and memory: II. extrinsic connections. J Comp Neurol 520:3338–3368.

Gollisch T, Meister M (2010) Eye smarter than scientists believed: neural computations in circuits of the retina. Neuron 65:150–164.

Grewe J, Kruscha A, Lindner B, Benda J (2017) Synchronous spikes are necessary but not sufficient for a synchrony code in populations of spiking neurons. PNAS 114:E1977–E1985.

Gussin D, Benda J, Maler L (2007) Limits of linear rate coding of dynamic stimuli by electroreceptor afferents. J Neurophysiol 97:2917–2929.

Hagedorn M (1988) Ecology and behavior of a pulse-type electric fish *Hypopomus occidentalis* in a fresh-water stream in Panama. Copeia 2:324–335.

Hagedorn M, Heiligenberg W (1985) Court and spark: electric signals in the courtship and mating of gymnotid fish. Anim Behav 33:254–265.

Heiligenberg W (1991) Neural nets in electric fish. Cambridge, MA: MIT Press.

Heiligenberg W, Dye J (1982) Labelling of electroreceptive afferents in a gymnotoid fish by intraeellular injection of HRP: the mystery of multiple maps. J Comp Physiol 148:287–296.

Hopkins CD (1973) Lightning as background noise for communication among electric fish. Nature 242:268–270.

Hupé GJ, Lewis JE (2008) Electrocommunication signals in free swimming brown ghost knifefish, *Apteronotus leptorhynchus*. J Exp Biol 211:1657–1667.

Jun JJ, Longtin A, Maler L (2013) Real-time localization of moving dipole sources for tracking multiple free-swimming weakly electric fish. PLoS ONE 8.

Jung SN, Longtin A, Maler L (2016) Weak signal amplification and detection by higher-order sensory neurons. J Neurophysiol 115:2158–2175.

Kirschbaum F, Schugardt C (2002) Reproductive strategies and developmental aspects in mormyrid and gymnotiform fishes. J Physiol Paris 96:557–566.

Knight BW (1972) Dynamics of encoding in a population of neurons. J Gen Physiol 59:734–766.

Knudsen EI (1974) Behavioral thresholds to electric signals in high frequency electric fish. J Comp Physiol A 91:333–353.

Kostarakos K, Hennig MR, Römer H (2009) Two matched filters and the evolution of mating signals in four species of cricket. Front Zool 6:22.

Krahe R, Bastian J, Chacron MJ (2008) Temporal processing across multiple topographic maps in the electrosensory system. J Neurophysiol 100:852–867.

Krahe R, Maler L (2014) Neural maps in the electrosensory system of weakly electric fish. Curr Opin Neurobiol 24:13–21.

Ladich F (2007) Females whisper briefly during sex: context- and sex-specific differences in sounds made by croaking gouramis. Anim Behav 73:379–387.

Laughlin S (1981) A simple coding procedure enhances a neuron's information capacity. Z Naturforsch C 36:910–912.

Lewicki MS, Olshausen BA, Surlykke A, Moss CF (2014) Scene analysis in the natural environment. Front Psychol 5:1–21.

Lobel PS (1992) Sounds produced by spawning fishes. Environ Biol Fishes 33:351–358.

Machens CK, Gollisch T, Kolesnikova O, Herz AVM (2005) Testing the efficiency of sensory coding with optimal stimulus ensembles. Neuron 47:447–456.

Maler L (2009a) Receptive field organization across multiple electrosensory maps. I. Columnar organization and estimation of receptive field size. J Comp Neurol 516:376–393.

Maler L (2009b) Receptive field organization across multiple electrosensory maps. II. Computational analysis of the effects of receptive field size on prey localization. J Comp Neurol 516:394–422.

Maler L, Finger T, Karten HJ (1974) Differential projections of ordinary lateral line receptors and electroreceptors in the gymnotid fish, *Apteronotus (Sternarchus) albifrons*. J Comp Neurol 158:363–382.

Maler L, Sas EKB, Rogers J (1981) The cytology of the posterior lateral line lobe of high-frequency weakly electric fish (Gymnotidae): Dendritic differentiation and synaptic specificity in a simple cortex. J Comp Neurol 195:87–139.

Markham MR, Ban Y, McCauley A, Maltby R (2016) Energetics of sensing and communication in electric fish: A blessing and a curse in the Anthropocene? Integr Comp Biol 56:889–900.

Marsat G, Longtin A, Maler L (2012) Cellular and circuit properties supporting different sensory coding strategies in electric fish and other systems. Curr Opin Neurobiol 22:1–7.

Metzner W, Heiligenberg W (1991) The coding of signals in the electric communication of the gymnotiform fish *Eigenmannia*: From electroreceptors to neurons in the torus semicircularis of the midbrain. J Comp Physiol A 169:135–150.

Metzner W, Juranek J (1997) A sensory brain map for each behavior? PNAS 94:14798–14803.

Meyer JH, Leong M, Keller CH (1987) Hormone-induced and maturational changes in electric organ discharges and electroreceptor tuning in the weakly electric fish *Apteronotus*. J Comp Physiol A 160:385–394.

Meyer JH, Zakon HH (1982) Androgens alter the tuning of electroreceptors. Science 217:635–637.

Middleton JW, Longtin A, Benda J, Maler L (2009) Postsynaptic receptive field size and spike threshold determine encoding of high-frequency information via sensitivity to synchronous presynaptic activity. J Neurophysiol 101:1160–1170.

Nelson ME, MacIver MA (1999) Prey capture in the weakly electric fish *Apteronotus albifrons*: sensory acquisition strategies and electrosensory consequences. J Exp Biol 202:1195–1203.

Nelson ME, Xu Z, Payne JR (1997) Characterization and modeling of P-type electrosensory afferent responses to amplitude modulations in a wave-type electric fish. J Comp Physiol A 181:532–544.

Olshausen BA, Field DJ (1996) Emergence of simple-cell receptive-field properties by learning a sparse code for natural images. Nature 381:607–609.

Olshausen BA, Field DJ (2005) How close are we to understanding V1?. Neural Comput 17:1665–1699.

Rieke F, Bodnar DA, Bialek W (1995) Naturalistic stimuli increase the rate and efficiency of information transmission by primary auditory afferents. Proc R Soc Lond B 262:259–265.

Rodriguez-Munoz R, Bretman A, Slate J, Walling CA, Tregenza T (2010) Natural and sexual selection in a wild insect population. Science 328:1269–1272.

Rose G, Heiligenberg W (1985) Temporal hyperacuity in the electric sense of fish. Nature 318:178–180.

Salazar VL, Krahe R, Lewis JE (2013) The energetics of electric organ discharge generation in gymnotiform weakly electric fish. J Exp Biol 216:2459–2468.

Salgado JAG, Zupanc GKH (2011) Echo response to chirping in the weakly electric brown ghost knifefish (*Apteronotus leptorhynchus*): role of frequency and amplitude modulations . Can J Zool 89:498–508.

de Santana CD, Vari RP (2013) Brown ghost electric fishes of the *Apteronotus leptorhynchus* species-group (Ostariophysi, Gymnotiformes); monophyly, major clades, and revision. Zool J Linnean Soc 168:564–596.

Savard M, Krahe R, Chacron MJ (2011) Neural heterogeneities influence envelope and temporal coding at the sensory periphery. Neurosci 172:270–284.

Scheich H, Bullock TH, Robert H Hamstra J (1973) Coding properties of two classes of afferent nerve fibers: high frequency electroreceptors in the electric fish, *Eigenmannia*. J Neurophysiol 36:39–60.

Schrode KM, Bee MA (2015) Evolutionary adaptations for the temporal processing of natural sounds by the anuran peripheral auditory system. J Exp Biol 218:837–848.

Silva A, Quintana L, Perrone R, Sierra F (2008) Sexual and seasonal plasticity in the emission of social electric signals. Behavioral approach and neural bases. J Physiol Paris 102:272–278.

Smith EC, Lewicki MS (2006) Efficient auditory coding. Nature 439:978–982.

Smith GT (2013) Evolution and hormonal regulation of sex differences in the electrocommunication behavior of ghost knifefishes (Apteronotidae). J Exp Biol 216:2421–33.

Stamper SA, Carrera-G E, Tan EW, Fugère V, Krahe R, Fortune ES (2010) Species differences in group size and electrosensory interference in weakly electric fishes: implications for electrosensory processing. Behav Brain Res 207:368–376.

Stöckl A, Sinz F, Benda J, Grewe J (2014) Encoding of social signals in all three electrosensory pathways of *Eigenmannia virescens*. J Neurophysiol 112:2076–2091.

Theunissen FE, Sen K, Doupe AJ (2000) Spectral-temporal receptive fields of nonlinear auditory neurons obtained using natural sounds. The Journal of Neuroscience 20:2315–2331.

Triefenbach FA, Zakon H (2008) Changes in signalling during agonistic interactions between male weakly electric knifefish, *Apteronotus leptorhynchus*. Anim Behav 75:1263–1272.

Vonderschen K, Chacron MJ (2011) Sparse and dense coding of natural stimuli by distinct midbrain neuron subpopulations in weakly electric fish. J Neurophysiol 106:3102–3118.

Walz H, Grewe J, Benda J (2014) Static frequency tuning properties account for changes in neural synchrony evoked by transient communication signals. J Neurophysiol 112:752–765.

Walz H, Hupé G, Benda J, Lewis JE (2013) The neuroethology of electrocommunication: how signal background influences sensory encoding and behaviour in *Apteronotus leptorhynchus*. J Physiol Paris 107:13–25.

Wilson EO (1975) Sociobiology: the new synthesis. Camridge MA: Harvard University Press.

Zakon HH, Oestreich J, Tallarovic S, Triefenbach F (2002) EOD modulations of brown ghost electric fish: JARs, chirps, rises, and dips. J Physiol Paris 96:451–458.

Zupanc GKH, Sîrbulescu RF, Nichols A, Ilies I (2006) Electric interactions through chirping behavior in the weakly electric fish, *Apteronotus leptorhynchus*. J Comp Physiol A 192:159–173.

Supporting information

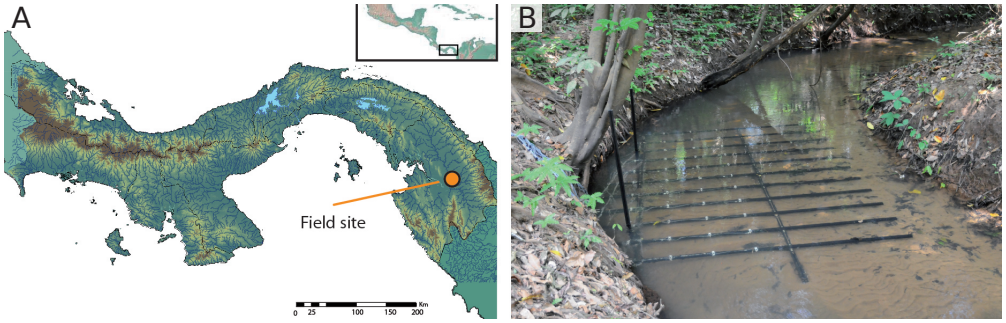

Figure S 1: Field site and position of electrode array. A) The field data were recorded in the Darin province in Eastern Panam. B) The electrode array covered $2.4 \times 1.5\,\mathrm{m}^2$ of our recording site in a small quebrada of the Chucunaque River system. Electrodes (on white electrode holders) were positioned partly beneath the excavated banks, allowing to record electric fish hiding deep in the root masses.

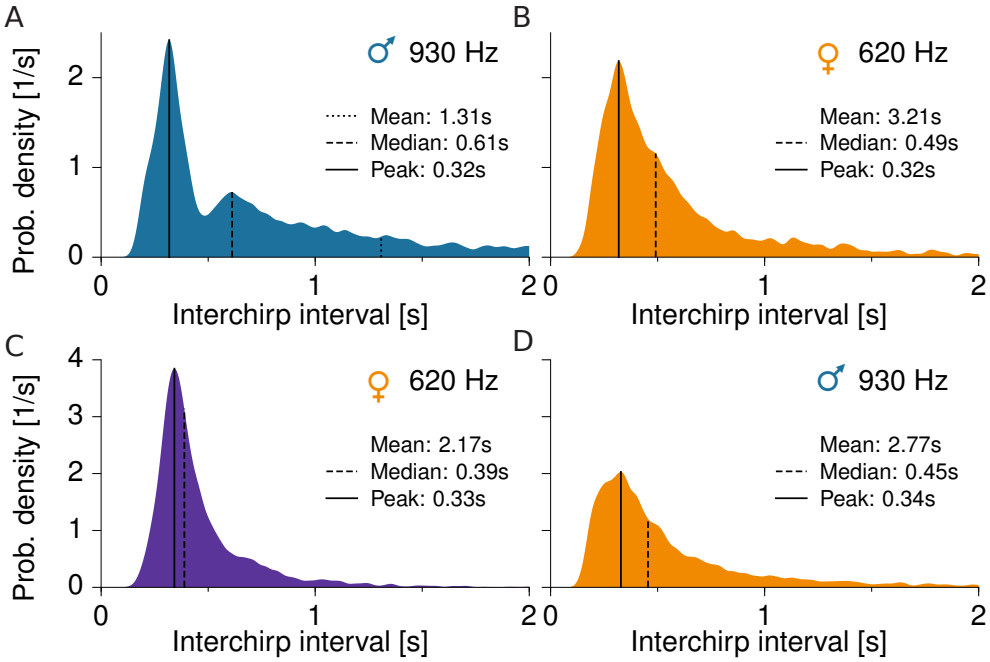

Figure S 2: Interchirp-interval distributions of small chirps of an example female (right column, EODf = 620 Hz; B: n = 3431, D: n = 5336 chirps) interacting with two males (left column; A: EODf = 930 Hz, n = 8439; C: EODf = 1035 Hz, n = 6857 chirps).

Audio, Animations, and Video

Audio S 3: Audio trace of the courtship sequence shown in Fig. 3. A male (EODf = 930 Hz) generated a series of small chirps. Eventually, the female (EODf = 620 Hz) fish joins in, increases chirp rate and finishes with a long chirp, which is acknowledged by the male with a small chirp doublet.

File: audio_courtship.wav

Movie S 4: Example of raw voltage recordings and corresponding position estimates of a single fish, *Eigenmannia humboldtii*, passing through the array of electrodes. The head and tail area of its electric field are of opposite polarity, which is why the polarity of the recorded EOD switches as the fish passes an electrode. Note the large electric spikes occurring irregularly on all electrodes. Previous studies (Hopkins, 1973) attributed similar patterns to propagating distant lightning. The animation is played back at real-time.

File: movie_raw_and_position.avi

Movie S 5: Animation of the courtship and aggression behavior shown in Fig. 2. A courting dyad is engaged in intense chirp activity (transparent circles and 50 ms beeps at the fish's baseline EODf). An intruder male (red circles indicate positions of the last 5 seconds, black circles mark current positions) first lingers at a distance of one meter. When it approaches further, courting is interrupted and the resident male engages the intruder. Just before the male intruder retreats, it emits a series of small chirps, and subsequently leaves the recording area. The resident male returns to the female and resumes chirping. Eventually, the female responds with small chirps followed by a single long chirp (large open circle and a 500 ms beep at the female's baseline EODf). Then both fish cease chirp activity and the male resumes to emit chirps after a few seconds. The animation is played back at 2× real-time.

File: movie_intruder.avi

Movie S 6: Animation of a courtship sequence with multiple attempts of an intruding male to approach the courting dyad. The resident male drives the intruder away three times , starting the approach at increasingly greater distances. *Apteronotus rostratus* are marked by circles, *Eigenmannia humboldtii* by squares. The animation is played back at $2\times$ real-time.

File: movie_repetitive_intruder.avi

Movie S 7: Spawning of the closely related species *Apteronotus lepthorhynchus* during a breeding experiment. The overall sequence of chirp production is very similar to the courtship motif observed in *A. rostratus*. However, male *A. lepthorhynchus* increasingly generate a second type of chirp, a variety of a long chirp, as spawning approaches. The video shows a big male (EOD$f = 770$ Hz) courting a smaller female (590 Hz). The audio signal was created from concurrent EOD recordings. Both fish generate chirps at an increased rate (about 1.5 Hz), just before the male thrusts its snout against the female, which responds with a long chirp, clearly noticeable from the audio trace. Subsequently, the male retreats to a tube and the female hovers around the substrate, where the spawned egg was found.

File: movie_spawning.avi